Design of Asymptotically Stable Walking for a 5-Link Planar Biped Walker via Optimization

E.R. Westervelt and J.W. Grizzle

Department of Electrical Engineering and Computer Science
The University of Michigan, Ann Arbor, MI, 48109-2110, USA
{ewesterv,grizzle}@umich.edu

Abstract— **Closed-loop, asymptotically stable walking motions are designed for a 5-link, planar bipedal robot model with one degree of underactuation. Parameter optimization is applied to the hybrid zero dynamics, a 1-DOF invariant subdynamics of the of the full robot model, in order to create asymptotically stable orbits. Tuning the dynamics of this 1 DOF subsystem via optimization is interesting because asymptotically stable orbits of the zero dynamics correspond to asymptotically stabilizable orbits of the full hybrid model of the walker. The optimization process uses a sequential quadratic programming (SQP) algorithm and is able to satisfy kinematic and dynamic constraints while approximately minimizing energy consumption and ensuring stability. This is in contrast with traditional approaches to the design of walking controllers where approximately optimal walking (time-) trajectories are derived and then enforced on the robot using a trajectory tracking controller.**

I. Introduction

For planar, biped walkers with a torso and one degree of under actuation, it was shown for the first time in [1] for a 3-link model, and in [2] for a 5-link model, that these systems admit feedback control designs that induce walking motions with provable stability properties. The system models are hybrid, consisting of ordinary differential equations to describe the motion of the robot when only one leg is in contact with the ground (single support or swing phase of the walking motion), and a discrete map to model the impact when the second leg touches the ground (double support phase). The control designs involved the judicious choice of a set of holonomic constraints that were imposed on the robot via feedback control. This was accomplished by interpreting the constraints as output functions depending only on the configuration variables of the robot, and then combining ideas from finite-time stabilization and computed torque. The desired posture of the robot was encoded into the set of outputs in a such a way that the nulling of the outputs was equivalent to achieving the desired posture. However, the choice of the outputs was *ad hoc* and did not lead to energy efficient walking motions.

The contribution of this paper is to provide a systematic methodology for choosing outputs that achieve stable walking motions that exploit as much as possible the natural dynamics of the system. The heart of the method is the application of parameter optimization to a 1-DOF subsystem of the full hybrid model of the robot, recently developed in [3]. In that work, it is shown that the zero dynamics of the swing phase [1] can be made invariant under the impact map, resulting in the definition of the *hybrid zero dynamics*, whose stability properties are directly relatable to the stabilizability of the orbits of the full hybrid system. The associated Poincaré return map of the hybrid zero dynamics was explicitly computed and shown to be diffeomorphic to a scalar, linear-time invariant system, thereby rendering transparent the existence and stability properties of periodic orbits of the hybrid zero dynamics. By parameter optimization on the hybrid zero dynamics, kinematic and dynamic constraints can be met while approximately minimizing energy consumption. The overall concept is similar to [4], with the difference that, in conjunction with the general feedback approach developed in [1, 2], an asymptotically stable orbit of the hybrid zero dynamics immediately yields a provably, asymptotically stable orbit in the full hybrid model.

The use of optimization in the analysis and design of biped walking motions is not a new concept. Work as early as the 1970's can be found in the biomechanics literature (see [5, 6], for example). In more recent years, the design of optimal or approximately optimal trajectories for biped robots has become a popular topic [4, 7–13]. In each case the approach has been to design time trajectories such that a defined cost is minimized, or approximately minimized, subject to a set of constraints. The employed optimization technique varies. Cabodevila and Abba [7] parameterized the robot state as a finite Fourier series and compared the performance of three algorithms: Nelder and Mead, Genetic, and Simulated Annealing. Chevallereau and Aoustin [4], and Chevallereau and Sardain [8] rewrote the controllable dynamics of the robot as a polynomial function of the uncontrolled dynamics and used Sequential Quadratic Pro-

gramming (SQP). Hasegawa, Arakawa, and Fukuda [9] used a modified genetic algorithm to generate reference trajectories parameterized as cubic splines. Hardt [10] used an optimization package, DIRCOL [14], which implements a sparse SQP algorithm and uses a variable number of cubic splines to approximate the state and associated control signals. Rostami and Bessonnet [12] applied Pontryagin's Maximum Principle. Roussel, Canudas-de-Wit, and Goswami [13] approximate the dynamics and use a direct shooting optimization algorithm. While the approach presented here uses the same optimization package as in [10], the result of the optimization is not an optimal or approximately optimal open-loop trajectory, but rather a *closed-loop system* which creates an asymptotically stable, invariant orbit, and along this orbit, energy consumption has been approximately minimized, while satisfying other natural kinematic and dynamic constraints.

Section II reviews the 5-link robot model studied here, though the results may be directly extended to the class of N-link models described in [3, 4]. Section III summarizes the work of [3] on the hybrid zero dynamics. Section IV presents a *new* class of output functions for which the hybrid zero dynamics may be computed in closed-form and conveniently parameterized. Section V uses optimization methods to shape the parameterized, hybrid zero dynamics so as to create asymptotically stable orbits.

II. Robot model and modeling assumptions

The robot, depicted in Figure 1, is assumed to be planar and consist of a torso and two identical legs with knees; furthermore, all links have mass, are rigid, and are connected in revolute joints. All walking cycles will be assumed to take place in the sagittal plane and consist of successive phases of *single support* (meaning the stance leg is touching the walking surface and the swing leg is not) and *double support* (the swing leg and the stance leg are both in contact with the walking surface). During the single support phase, it is assumed that the stance leg acts as a pivot. It is further supposed that the walking gaits of interest are such that successive phases of single support are symmetric, and progress from left to right.

The two phases of the walking cycle naturally lead to a mathematical model of the biped consisting of two parts: the differential equations describing the dynamics during the single support phase, and a model of the contact event. The rigid contact model of [15] is assumed, which collapses the double support phase to an instant in time, and allows a discontinuity in the velocity component of the state, with the position remaining continuous. The biped model is thus *hybrid* in nature, consisting of a continuous dynamics and a re-initialization rule at the contact event.

Model parameters	Torso (T)	Femurs (f)	Tibias (t)
Mass (kg)	20	6.8	3.2
L_* (m)	0.625	0.4	0.4
Inertia (m^2kg)	2.22	1.08	0.93
p_*^M (m)	0.2	0.163	0.128

TABLE I
Model parameters

Swing phase model: With 5-links, the dynamic model of the robot during the swing phase has 5-DOF. Let $q = (q_1, \cdots, q_5)'$ be the set of coordinates depicted in Figure 1, which describe the configuration of the robot with respect to the world reference frame W. Since only symmetric gaits are of interest, the same model can be used irrespective of which leg is the stance leg if the coordinates are relabeled after each phase of double support. Using the method of Lagrange, the model is written in the form

$$D(q)\ddot{q} + C(q,\dot{q})\dot{q} + G(q) = Bu. \tag{1}$$

Table I lists the associated model parameters (see Figures 2 and 3 for details on the parameter definitions used here; the inertias listed here include the rotor inertia reflected through the gear reducer). Torques u_i, $i = 1$ to 4, are applied between each connection of two links, *but not between the stance leg and ground.* The model is written in state space form by

$$\begin{aligned} \dot{x} &= \begin{bmatrix} \dot{q} \\ D^{-1}(q)\left[-C(q,\dot{q})\dot{q} - G(q) + Bu\right] \end{bmatrix} \\ &=: f(x) + g(x)u. \end{aligned} \tag{2}$$

where $x := (q', \dot{q}')'$. The state space of the model is taken as $\mathcal{X} := \{x := (q', \dot{q}')' \mid q \in \mathcal{Q},\ \dot{q} \in I\!R^5\}$, where $\mathcal{Q}$ is a simply-connected, open subset of $[0, 2\pi)^5$ corresponding to physically reasonable configurations of the robot, as done in [2].

Impact model: An impact occurs when the swing leg touches the walking surface, $S := \{(q,\dot{q}) \in \mathcal{X} \mid p_2^v = 0,\ p_2^h > 0\}$, also called the ground. The impact between the swing leg and the ground is modeled as a contact between two rigid bodies. In addition to modeling the change in state of the robot, the impact model accounts for the relabeling of the robot's coordinates that occurs after each phase of double support. Let R be the constant matrix such that $R \cdot q$ accounts for relabeling of the coordinates when the swing leg becomes the new stance leg. Then the impact model of [15] under standard hypotheses (see [1], for example), results in a smooth map $\Delta : S \to \mathcal{X}$,

$$x^+ = \Delta(x^-), \tag{3}$$

where $x^+ := (q^+, \dot{q}^+)$ (resp. $x^- := (q^-, \dot{q}^-)$) is the state value just after (resp. just before) impact. For later convenience, Δ is expressed as

$$\Delta(x^-) := \begin{bmatrix} \Delta_q \cdot q^- \\ \Delta_{\dot{q}}(q^-) \cdot \dot{q}^- \end{bmatrix} \tag{4}$$

where $\Delta_q := R$ and $\Delta_{\dot{q}}(q)$ is a 5×5 matrix of smooth functions of q.

Nonlinear system with impulse effects: The overall biped robot model can be expressed as a nonlinear system with impulse effects [16]

$$\begin{array}{rcll} \dot{x} & = & f(x) + g(x)u & x^- \notin S \\ x^+ & = & \Delta(x^-) & x^- \in S, \end{array} \tag{5}$$

where, $x^-(t) := \lim_{\tau \nearrow t} x(\tau)$. Solutions are taken to be right continuous and must have finite left and right limits at each impact event (see [1] for details).

A *half-step* of the robot is defined to be a solution of (5) that starts with the robot in double support, ends in double support with the positions of the legs swapped, and contains no other impact event.

III. Summary of hybrid zero dynamics

In general, the *maximal internal dynamics of a system that are compatible with the output being identically zero* is called the *zero dynamics* [17]. In [3], this notion was extended to include the impact map common in many biped models. This section briefly summarizes the main results [3], and due to space limitations, assumes familiarity with the zero dynamics of non-hybrid models.

Consider first the swing phase dynamics, (2), and note that if an output $y = h(q)$ depends only on the position variables, then, due to the second order nature of the robot model, the derivative of the output along solutions of (2) does not depend directly on the inputs. Hence its relative degree is at least two. Differentiating the output once again computes the accelerations, resulting in

$$\frac{d^2 y}{dt^2} = L_f^2 h(q, \dot{q}) + L_g L_f h(q) u, \tag{6}$$

where the matrix $L_g L_f h(q)$ is called the decoupling matrix and depends only on the configuration variables. A consequence of the general results in [17] is that the invertibility of this matrix at a given point assures the existence and uniqueness of the zero dynamics in the neighborhood of that point. With a few extra hypotheses, these properties can be assured on a given open set.

Output function hypotheses: The output functions considered are assumed to be smooth functions satisfying the following hypotheses:

HH1) h is a function of only the position coordinates;

HH2) there exists an open set $\tilde{\mathcal{Q}} \subset \mathcal{Q}$ such that for each point $q \in \tilde{\mathcal{Q}}$, the decoupling matrix $L_g L_f h(q)$ is square and invertible (i.e., h has vector relative degree $(2, \ldots, 2)'$);

HH3) there exists a smooth real valued function $\theta(q)$ such that $\Phi : \tilde{\mathcal{Q}} \to \mathbb{R}^5$ by $\Phi(q) := (h(q)', \theta(q))'$ is a diffeomorphism onto its image;

HH4) there exists a unique point $q^- \in \tilde{\mathcal{Q}}$ such that $(h(q^-), p_2^v(q^-)) = (0, 0)$ and the rank of $[h',\ p_2^v]'$ at q^- equals 5.

Swing phase zero dynamics (cf. [3, Theorem 2]): Hypotheses HH1–HH4 ensure that $Z := \{x \in \tilde{\mathcal{Q}} \times \mathbb{R}^N \mid h(x) = 0, L_f h(x) = 0\}$ is a smooth two dimensional submanifold of $\mathcal{X}$; moreover, the feedback control

$$u^*(x) = -(L_g L_f h(x))^{-1} L_f^2 h(x) \tag{7}$$

renders Z invariant under the swing phase dynamics in the sense that, every $z \in Z$, $f_{zero}(z) := f(z) + g(z)u^*(z) \in T_z Z$. Z is called the *zero dynamics manifold* and $\dot{z} = f_{zero}(z)$ is called the (swing phase) *zero dynamics*.

Hybrid zero dynamics (cf. [3, Theorem 5]): Requiring that the swing phase dynamics be invariant under the impact map, that is, $\Delta(S \cap Z) \subset Z$, results in the *hybrid zero dynamics*,

$$\begin{array}{rcll} \dot{z} & = & f_{zero}(z) & z^- \notin S \cap Z \\ z^+ & = & \Delta(z^-) & z^- \in S \cap Z. \end{array} \tag{8}$$

It is shown in [3] that along all solutions of (8), the output h is identically zero, hence this is a valid zero dynamics for the hybrid model. Let θ be as in HH3 and let γ_0 be the last row of D. Then in the local coordinates, $(\xi_1, \xi_2) := (\theta(q), \gamma_0(q) \cdot \dot{q})$, the swing phase zero dynamics of (2) become

$$\begin{array}{rcl} \dot{\xi}_1 & = & \alpha(\xi_1)\xi_2 \\ \dot{\xi}_2 & = & \beta(\xi_1) \end{array} \tag{9}$$

where α and β are smooth functions of ξ_1. Furthermore, $S \cap Z$ can be shown to be diffeomorphic to $\mathbb{R}$ per $\sigma : \mathbb{R} \to S \cap Z$, where $\sigma(\omega) := [\sigma_q',\ (\sigma_{\dot{q}} \cdot \omega)']'$, $\sigma_q := q^-$,

$$\sigma_{\dot{q}} := \begin{bmatrix} \frac{\partial h}{\partial q}(q^-) \\ \gamma_0(q^-) \end{bmatrix}^{-1} \begin{bmatrix} 0 \\ 1 \end{bmatrix}, \tag{10}$$

and q^- is given by HH4. In addition, θ, when evaluated along any half step of the zero dynamics, is a strictly monotonic function of time and thus achieves its maximum and minimum values at the end points. Thus, the extrema of $\theta(q)$ over a half step are $\theta^- := \theta(q^-)$ and $\theta^+ := \theta(\Delta_q(q^-))$. Without loss of generality, it is assumed that $\theta^+ < \theta^-$; that is, that along

any half-step of the hybrid zero dynamics, θ is *monotonically increasing*.

Poincaré analysis of the zero dynamics (cf. [3, Theorem 7]) Assume that a smooth output function h on (5) satisfies HH1–HH4 function, and take the Poincaré section to be $S \cap Z$ so that the Poincaré map is the partial map $\rho : S \cap Z \to S \cap Z$ defined as in [1]. In local coordinates $(\zeta_1, \zeta_2) := (\theta(q), \frac{1}{2}(\gamma_0(q)\cdot\dot{q})^2)$, the Poincaré map can be explicitly computed. Indeed, $\Delta : (\zeta_1^-, \zeta_2^-) \to (\zeta_1^+, \zeta_2^+)$ is $\zeta_1^+ = \theta^+$ and $\zeta_2^+ = \delta_{zero}^2 \cdot \zeta_2^-$, where $\delta_{zero} := \gamma_0(q^+) \cdot \Delta_{\dot{q}}(q^-) \cdot \sigma_{\dot{q}}(q^-)$, a constant that may be computed *a priori*. In these coordinates, the hybrid zero dynamics (9) may be integrated to obtain

$$\rho(\zeta_2^-) = \delta_{zero}^2 \cdot \zeta_2^- + \kappa(\theta^-), \tag{11}$$

where for $\theta^+ \le \zeta_1 \le \theta^-$,

$$\kappa(\zeta_1) := \int_{\theta^+}^{\zeta_1} \frac{\beta(\zeta)}{\alpha(\zeta)} \cdot d\zeta. \tag{12}$$

The domain of definition of (11) is

$$\left\{\zeta_2^- > 0 \mid \delta_{zero}^2 \cdot \zeta_2^- + K \ge 0\right\}. \tag{13}$$

where $K := \min_{\theta^+ \le \xi_1 \le \theta^-} \kappa(\zeta_1)$.

If $\delta_{zero}^2 \neq 1$ and $\zeta_2^* := \kappa(\theta^-)/(1 - \delta_{zero}^2)$ is in the domain of definition of ρ, then it is the unique fixed point of ρ. Moreover, if ζ_2^* is a fixed point, then ζ_2^* is an asymptotically stable equilibrium point of

$$\zeta_2(k+1) = \rho(\zeta_2(k)) \tag{14}$$

if, and only if, $\delta_{zero}^2 < 1$, and in its domain of attraction is (13), that is, the entire domain of definition of ρ.

While the domain of definition of the Poincaré map is (13), not all solutions of the zero dynamics satisfy the modeling assumptions. In particular, the assumption that the stance leg acts as a pivot during the swing phase limits the ratio and sign of the ground reaction forces on the stance leg end. This limit can be reflected as an upper bound on the mathematical domain of definition of ρ; see [18]. In Section V, this will be taken care of through the imposition of an appropriate constraint.

IV. An almost linear output structure

Consider the following output function and form for $\theta(q)$

$$\begin{aligned} y = h(q) &:= Aq - b(\theta(q)) && (15)\\ \theta(q) &= cq && (16)\end{aligned}$$

where $A : \mathbb{R}^5 \to \mathbb{R}^4$ is a linear map, $c : \mathbb{R}^5 \to \mathbb{R}$ is a linear functional, and $b : \mathbb{R} \to \mathbb{R}^4$ is a to-be-specified smooth function. Driving y to zero will force the chosen linear combinations of the generalized coordinates to track $b(\theta(q))$. Intuitively, the posture of the robot is being controlled as a holonomic constraint parameterized by the uncontrolled quantity $\theta(q)$.

By specializing b as a vector of Bézier polynomials, it turns out to be easy to enforce the invariance condition, $\Delta(S \cap Z) \subset Z$, which is required for the existence of a non-trivial hybrid zero dynamics. This is developed next. A one-dimensional Bézier polynomial [19] of degree M is a polynomial, $b_i : [0,1] \to \mathbb{R}$, defined by $M+1$ coefficients, $a_{k,i}$, per

$$b_i(s) := \sum_{k=0}^{M} a_{i,k} \cdot \frac{M!}{k!(M-k)!} \cdot s^k (1-s)^{M-k}. \tag{17}$$

Some particularly useful features of Bézier polynomials are (see [20, page 291])

1. the image of the Bézier polynomial is contained in the convex hull of the $M+1$ control points (as viewed as points in $\mathbb{R}^2$, $\{(0, a_{i,0})$, $(1/M, a_{i,1})$, $(2/M, a_{i,2}), \ldots,$ $(1, a_{i,M})\}$) (the polynomial does not exhibit large oscillations with small parameter variations as can happen with a polynomial with a standard parameterization);
2. $b_i(0) = a_{i,0}$ and $b_i(1) = a_{i,M}$; and
3. the two lines defined by the pairs of points

$$\{(0, a_{i,0}), (1/M, a_{i,1})\}$$

and

$$\{(1 - 1/M, a_{i,M-1}), (1, a_{i,M})\}$$

are tangent to $b_i(s)$ at $(0, a_{i,0})$ and $(1, a_{i,M})$, respectively.

The first feature will be useful for numerical calculations (such as approximating the gradient of a cost function) where numerical stability is crucial. The second two features are exactly those used to achieve $\Delta(S \cap Z) \subset S$.

The function $\theta(q)$ of the generalized coordinates will not, in general, take values in the unit interval over a phase of single support. Therefore, to appropriately compose a Bézier polynomial with $\theta(q)$, it is necessary to normalize θ by

$$\bar{\theta}(q) := \frac{\theta(q) - \theta^+}{\theta^- - \theta^+}, \tag{18}$$

which takes values in $[0,1]$. Define $\bar{b}_i(\theta(q)) := b_i(\bar{\theta}(q))$, and

$$b(\theta(q)) := \left(\bar{b}_1(\theta(q)), \cdots, \bar{b}_4(\theta(q))\right)'. \tag{19}$$

Setting

$$\begin{aligned} a_0 &:= (a_{1,0}, \ldots, a_{4,0})' \\ a_1 &:= (a_{1,1}, \ldots, a_{4,1})' \\ a_M &:= (a_{1,M}, \ldots, a_{4,M})' \end{aligned} \tag{20}$$

and evaluating (19) and its derivative with respect to θ at the beginning (resp. end) of a phase of single support, when $\theta(q) = \theta^+$ (resp. $\theta(q) = \theta^-$), leads to the following theorem.

Theorem 1: (see [18] for a proof of this theorem.) Consider the model (5) assume the existence of a smooth output h of the form (15), with b given by (19) and $\theta(q)$ given by (16), such that hypotheses HH1–HH4 hold. Then, $\Delta(S \cap Z) \subset Z$ if, and only if,

$$\begin{bmatrix} a_0 \\ \theta^+ \end{bmatrix} = \bar{A}R^{-1}\bar{A}^{-1} \begin{bmatrix} a_M \\ \theta^- \end{bmatrix} \tag{21}$$

and

$$a_1 = \frac{\theta^- - \theta^+}{Mc\dot{q}^+} \cdot A\dot{q}^+ + a_0 \tag{22}$$

where $\dot{q}^- = \sigma_{\dot{q}}(q^-)$ and $\dot{q}^+ := \Delta_{\dot{q}}(q^-) \cdot \dot{q}^-$. □

V. Creating Asymptotically Stable Fixed Points Through Optimization

Consider the system (5) with output (15), where b is defined by (19), $A = [I, 0]$ and $c = (0,\ 0,\ 1/2,\ 0,\ 1)$. Choosing $M = 6$ and imposing (21) and (22) leaves five free parameters for each output component. The goal now is to use optimization to select the free parameters so as to create an asymptotically stable fixed point of the hybrid zero dynamics, while meeting other natural objectives, such as low energy consumption, a desired walking speed, etc. The control torques needed to evolve along the zero dynamics manifold are given in closed-from by (7), and to compute these it is only necessary to solve the 1-DOF hybrid zero dynamics instead of the 5-DOF full model of the robot.

The optimization will be implemented with DIRCOL[1], which is able to handle nonlinear inequality constraints (NIC's), nonlinear boundary equality constraints (NBEC's), and explicit boundary constraints (EBC's). The NIC's must be satisfied at each point in the time interval of optimization; the NBEC's only need to be satisfied at the end of the interval of optimization; and the EBC's are always satisfied at the end of the interval of optimization. Unfortunately, DIRCOL does not handle EBC's at the beginning of the interval of optimization (see NBEC3 below).

Consider the hybrid zero dynamics (8) with cost function

$$J(a) := \frac{1}{p_2^h(T^-)} \int_0^{T^-} \sum_{i=1}^{4} (u_i^*(t))^2 dt, \tag{23}$$

where T^- is the time for a half-step, $p_2^h(T^-)$ corresponds to step length, and $u_i(t)$ is the result of evaluating (7) along a solution of the hybrid zero dynamics. The total number of parameters for optimization is $4(M-1)+1$, $M-1$ for each output[2] and ζ_2^*. DIRCOL requires the optimization problem be expressed in Mayer form, yielding

$$\dot{x}_1 = \alpha(x_1) \cdot x_2 \tag{24}$$

$$\dot{x}_2 = \beta(x_1) \tag{25}$$

$$\dot{x}_3 = \sum_{i=1}^{4} (u_i^*(x_1, x_2))^2. \tag{26}$$

Nonlinear Inequality Constraints: There are six NIC's that describe the desired walking motion per constraints on

NIC1) deflection of the stance leg knee;
NIC2) deflection of the swing leg knee;
NIC3) minimum hip height;
NIC4) minimum normal ground reaction force;
NIC5) maximum ratio of tangential to normal ground reaction forces experienced by the stance leg end; and
NIC6) swing foot height to ensure S intersects Z only the end of the step,

and two more dealing with existence and stability of a fixed point of the zero dynamics

NIC7) $\delta_{zero}^2 < 1$; and
NIC8) $\zeta_2^* > -K/\delta_{zero}^2$.

The first three NIC's ensure that the walking pattern will be similar to that of a human, while the next three enforce modeling assumptions.

Nonlinear Boundary Equality Constraints: There are five NBEC's that enforce

NBEC1) the desired walking rate;
NBEC2) that the post-impact velocity of the swing leg is positive;
NBEC3) the optimization state at $t = 0$ is such that $\theta(q) = \theta^+$;
NBEC4) the fixed point of the Poincaré map; and
NBEC5) the validity of the impact of the swing leg end with the walking surface.

Explicit Boundary Constraints: The two EBC's give the first two states when $t = T^-$,

EBC1) $x_1(T^-) = c \cdot \sigma_q$ and
EBC2) $x_2(T^-) = \gamma \circ \sigma(\zeta_2^*)$.

Note that without use of the hybrid zero dynamics there would be 10 states, the derivative of the cost, and four control signals to be included in the problem formulation, while stability of the closed-loop system would be hard to quantify and include as a simple optimization constraint. After optimization, hypothesis HH2, the invertibility of the decoupling matrix, is checked by using the technique presented in [2].

[1] `http://www.sim.informatik.tu-darmstadt.de/sw/dircol`

[2] By Theorem 1 two parameters per output can be calculated from the other $M-1$.

$J(a)$ (N^2m)	ζ_2^* $(kgm^2/s)^2$	δ^2_{zero} -	$\kappa(\theta^-)$ $(kgm^2/s)^2$	K $(kgm^2/s)^2$
36.79	978.8	0.638	354.4	-260.4

TABLE II

Optimization result statistics

Table II summarizes the result of optimization for a desired rate of 1.05 m/s. The walking motion is asymptotically stable since $\delta^2_{zero} < 1$ and $\zeta_2^* > -K/\delta^2_{zero} = 408.2$. Figure 4 is a stick figure animation of this result for a single half-step. The walking motion appears to be natural.

Acknowledgments

This work was supported in part by NSF grants INT-9980227 and IIS-9988695, and in part by the University of Michigan Center for Biomedical Engineering Research (CBER).

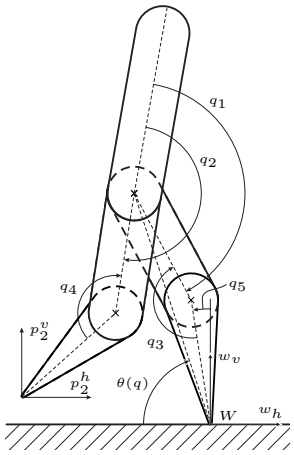

Fig. 1. Schematic of the 5-link robot considered with measurement conventions.

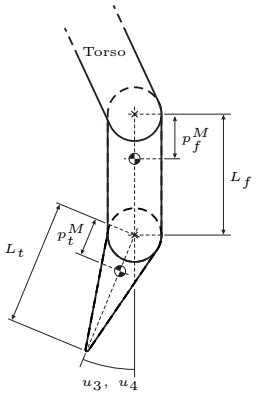

Fig. 2. Schematic of leg with measurement conventions.

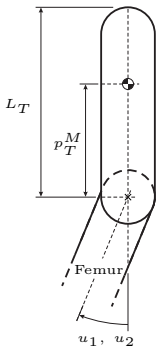

Fig. 3. Schematic of torso with measurement conventions.

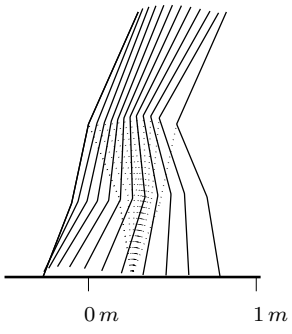

Fig. 4. Stick animation of robot taking one half-step from left to right. Note that the stance leg is dotted.

References

[1] J.W. Grizzle, G. Abba, and F. Plestan, "Asymptotically stable walking for biped robots: Analysis via systems with impulse effects," *IEEE Transactions on Automatic Control*, vol. 46, pp. 51–64, January 2001.

[2] F. Plestan, J.W. Grizzle, E.R. Westervelt, and G. Abba, "Stable walking of a 7-dof biped robot," in *Submitted to IEEE Transactions on Robotics and Automation*, February 2001.

[3] E. Westervelt, J. Grizzle, and D. Koditschek, "Zero dynamics of planar biped walkers with one degree of under actuation," in *IFAC 2002, Bareclona, Spain*, July 2002, Pre-print.

[4] C. Chevallereau and Aoustin, "Optimal reference trajectories for walking and running of a biped robot," *Robotica*, vol. 19, no. 5, pp. 557–569, September 2001.

[5] C.K. Chow and D.H. Jacobson, "Studies of human locomotion via optimal programming," *Mathematical Biosciences*, vol. 10, pp. 239–306, 1971.

[6] H. Hatze, "The complete optimization of a human motion," *Mathematical Biosciences*, vol. 28, pp. 99–135, 1976.

[7] G. Cabodevilla and G. Abba, "Quasi optimal gait for a biped robot using genetic algorithm," in *Proc. of the IEEE International Conference on Systems, Man and Cybernetics, Computational Cybernetics and Simulationms, Orlando, FL*, October 1997, pp. 3960–3965.

[8] C. Chevallereau and P. Sardain, "Design and actuation optimization of a 4 axes biped robot for walking and running," in *Proc. of the IEEE International Conference on Robotics and Automation, San Francisco, California*, April 2000, pp. 3365–3370.

[9] Y. Hasegawa, T. Arakawa, and T. Fukuda, "Trajectory generation for biped locomotion," *Mechatronics*, vol. 10, no. 1–2, pp. 67–89, March 2000.

[10] M.W. Hardt, *Multibody dynamical Algorithms, Numerical Optimal Control, with Detailed Studies in the Control of Jet Engine Compressors and Biped Walking*, Ph.D. thesis, University of California, San Diego, 1999.

[11] M. Rostami and G. Bessonnet, "Sagittal gait of a biped robot during the single support phase. part 1: passive motion," *Robotica*, vol. 19, pp. 163–176, March–April 2001.

[12] M. Rostami and G. Bessonnet, "Sagittal gait of a biped robot during the single support phase. part 2: optimal motion," *Robotica*, vol. 19, pp. 241–253, May–June 2001.

[13] C. Roussel, C. Canudas-de Wit, and A. Goswami, "Generation of energy optimal complete gait cycles for biped robots," in *Proc. of the IEEE International Conference on Robotics and Automation, Leuven, Belgium*, May 1998, pp. 2036–2041.

[14] O. von Stryk, *DIRCOL User's Guide*, Technische Universität Müchen, Zentrum Mathematik (SCB), Lehrstuhl M2 Höhere Mathematik und Numerische Mathematik, D-80290, Müchen, Germany, 2.1 edition, 1999.

[15] Y. Hurmuzlu and D.B. Marghitu, "Rigid body collisions of planar kinematic chains with multiple contact points," *International Journal of Robotics Research*, vol. 13, no. 1, pp. 82–92, 1994.

[16] H. Ye, A.N. Michel, and L. Hou, "Stability theory for hybrid dynamical systems," *IEEE Transactions on Automatic Control*, vol. 43, no. 4, pp. 461–474, April 1998.

[17] A. Isidori, *Nonlinear Control Systems: An Introduction*, Springer-Verlag, Berlin, third edition, 1995.

[18] E. Westervelt, J. Grizzle, and D. Koditschek, "Hybrid zero dynamics of n-link planar biped walkers," *In preparation*, 2001.

[19] P. Bézier, *Numerical Control: Mathematics and Applications*, John Wiley & Sons, New York, 1972.

[20] D.F. Rogers and J.A. Adams, *Mathematical Elements for Computer Graphics*, McGraw-Hill, New York, second edition, 1990.